Proceedings of the ICBBG2025
2025 International conference on Bio-mediated and Bio-inspired Geotechnics
18-20 May, 2025 | Tempe, Arizona, USA
https://doi.org/10.53243/ICBBG2025-61

ICBBG 18-20 May 2025

Effects of Biocementation Treatment on Mitigating Liquefaction-Induced Foundation Settlements Using 1g Shake Table Test

Md Kausar Alam,[1] Ramin Motamed, Ph.D., P.E., M.ASCE,[2] and Ben Ma, Ph.D.,[3]

[1]Department of Civil and Environmental Engineering, University of Nevada Reno, 1664 N Virginia St, Reno, NV 89557; E-mail: manik@unr.edu
[2]Department of Civil and Environmental Engineering, University of Nevada Reno, 1664 N Virginia St, Reno, NV 89557; E-mail: motamed@unr.edu
[3]Department of Civil and Environmental Engineering, University of Nevada Reno, 1664 N Virginia St, Reno, NV 89557; E-mail: benma@unr.edu

ABSTRACT

This research investigates the use of Microbially Induced Calcite Precipitation (MICP) to improve the engineering characteristics of granular soils through calcium carbonate deposition. The MICP was specifically used to reduce shallow foundation settlements caused by liquefaction during seismic activity. To accomplish these objectives, scaled model shake table tests are conducted, which were designed based on a large-scale shake table experiment carried out by our research team in 2018, and comprised three distinct soil layers with different relative densities. A shallow foundation was positioned on the upper crust layer, and the soil beneath the foundation was treated to achieve a shear wave velocity of 250 m/s. The experimental results demonstrated that MICP significantly decreased the time required for the dissipation of excess pore water pressure (PWP), as well as reduced foundation settlement and tilting. The reductions observed included a 50% decrease in the dissipation time of excess PWP, a 64% decrease in foundation settlement, and a 95% decrease in foundation tilting.

INTRODUCTION

Widespread liquefaction occurred in Japan during the 2011 Tohoku Earthquake, also referred to as the Great East Japan Earthquake Disaster, where the failure of shallow foundations underscored the impact of soil liquefaction in causing damage through ground deformations (Ishihara et al. 2014). Ecemis et al. (2023) investigated the impact of soil liquefaction on building performance during two earthquakes in southeastern Türkiye: the Kahramanmaraş-Pazarcık (M_w=7.8) and Kahramanmaraş-Elbistan (M_w=7.6) events. Their report revealed that numerous shallow foundations experienced excessive settlements and bearing capacity failures, including punching failure and building overturning. However, with the rising demand for construction sites, the need to improve the stability of existing grounds is increasing. Traditional methods such as chemical admixtures and reinforcement have harmful impacts on the environment. Naeimi and Haddad (2018) compared the environmental impact of soil improvement methods, including cement grouting and biocementation. The findings showed that calcium usage in cement grouting was 2.5 times higher than in bio-treated samples for achieving 700kPa unconfined compressive strength, resulting in greater energy consumption and higher gas emissions. This highlights MICP as potentially more environmentally friendly than traditional ground improvement techniques, such as Portland cement and polymer-based treatments.

MICP has the potential to improve the strength and stiffness of soils, resulting in increased liquefaction resistance and a reduction in reconsolidation settlements relative to untreated soils (Montoya et al., 2013; Darby et al. 2019). San Pablo et al. (2024) also conducted a centrifuge test to investigate the effect of treatment extent on the seismic performance of the system by varying the depth of improvement while keeping the same cross-sectional area. The test results revealed that total settlements of the surface increased as the improvement depth increased. Zamani et al. (2021) conducted centrifuge tests to investigate the mechanism of shallow foundation settlement in liquefiable soils treated with the MICP soil improvement technique. The test results revealed that MICP-treated zones significantly reduced both total and differential settlements of shallow foundations, with greater reductions observed as the treatment depth increased. However, there have been very few studies using 1g shake table tests to assess the effectiveness of MICP in mitigating liquefaction-induced foundation settlement.

The objective of this research was to perform 1g shake table tests to evaluate the effectiveness of MICP treatment in enhancing liquefaction resistance and reducing total and differential settlement of shallow foundations. Two 1g shake table tests were conducted using identical input motions, one with and one without the application of MICP treatment. Conclusions were then drawn based on the results of these tests.

MODEL PREPARATION

Iai (1989) introduced the similitude law that defines the relationship between prototype and model scales. In this study, we used the large-scale shake table experiments conducted by Orang et al. (2021) at the University of California, San Diego as the prototype. The prototype consisted of three distinct soil layers with varying relative densities: a top crust layer with 50% relative density, a middle liquefiable layer with 30% relative density, and a dense bottom layer with 85% relative density. To create a scaled-down model, we applied a scaling factor of 5, considering the feasibility of fitting the model within the dimensions of the soil box, which measures 204 cm in length, 64 cm in width, and 82 cm in height (Toth and Motamed, 2017; Alam et al., 2023; Alam and Motamed, 2024). The properties of both the prototype and the scaled model are calculated and presented in Table 1.

Table 1. The physical properties of the model ground in the model and prototype scale

Property	Ratio (Prototype/Model)	Model in this study (N=5)	Prototype (Orang et al. 2021)
Soil layer thickness (cm)	N	58	290
Foundation size (cm)	N	L (26) × W (12) × H (8)	130 × 60 × 40
Superstructure load (kg)	N^3	26.24	3279.47
Peak acceleration (g)	1	0.53	0.53
Frequency (Hz)	$N^{-0.75}$	6.68	2

*(L=Length, W= Width, H= Height) **

The model ground for the experiment was constructed using poorly graded #60 Monterey sand with the following physical properties: specific gravity G_s=2.65, maximum void ratio

e_{max}=0.78, minimum void ratio e_{min}=0.54, coefficient of curvature C_c=1.03, coefficient of uniformity C_u=1.65. The thickness of each soil layer was determined using similitude law, resulting in a 12 cm top crust layer, a 26 cm liquefiable layer, and a 20 cm dense layer. The base (dense) layer was first prepared in the soil box. The initial 5 cm of this layer was compacted with 5% moisture content to achieve a relative density of 85%. Then, an additional 15 cm of sand was added, and the entire base layer was gradually saturated from the bottom. The liquefiable layer, 26 cm thick, was constructed using the water pluviation method, with a constant particle fall height and a controlled water depth of 10 cm to ensure full saturation and removal of pore air. The water table was maintained at the top of the liquefiable layer throughout the process. The top crust layer was prepared using the air pluviation method. The foundation was placed on the soil model after the crust reached a thickness of 4 cm and achieved an approximate relative density of 50%. An additional 8 cm of the crust layer was added, resulting in a total thickness of 12 cm. A structural load of 26.24 kg was applied to the foundation. Throughout the experiment, 10 accelerometers, 2 PWP sensors, and 4 linear variable differential transformers (LVDTs) were used to monitor acceleration, excess PWP, foundation settlement, and free field conditions. The locations of these sensors are shown in Figure 1.

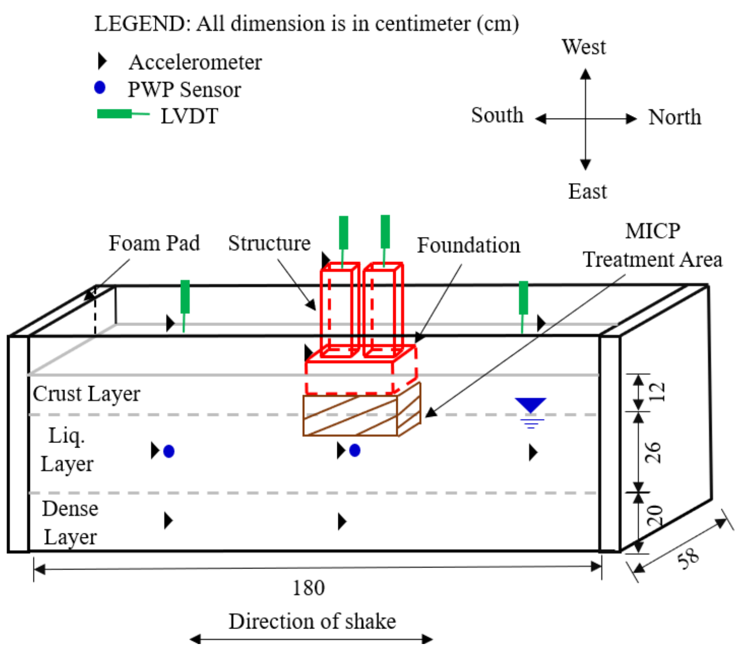

Figure 1. Schematic view of model box, model ground, foundation, structure and MICP treatment area

In this study, *Sporosarcina pasteurii (S. pasteurii),* a ureolytic soil bacteria, was used to establish the ureolytic activity in the sand. MICP treatment followed the procedures, chemical, and bacterial concentrations described by San Pablo et al. (2024). In our study, we planned to treat a single sand block with dimensions of 26 × 12 × 12 cm. The length and width of the block were similar to the foundation's length and width, while the block's thickness was 12 cm, compared to the foundation's thickness of 8 cm. By adopting this size, it is anticipated that the treatment block will cover 70% of the pressure bulb beneath the foundation, as indicated by the Boussinesq load distribution chart (Das and Sivakugan, 2018). A thin steel container measuring 26 × 12 × 20 cm was made for the treatment of the MICP block, as illustrated in Figure 2a. The container consists of a two-fold design, with a detachable inner section and a fixed, impervious outer section, as shown in Figure 2b. To facilitate the lifting of the treated soil, a geotextile was placed between the inner and outer sections of the mold. Inside the mold, a 12 cm layer of Monterey sand with a relative density (RD) of 40% was placed. The treatment solution was then injected into the soil, with the injection direction shown in Figure 3.

Measuring shear wave velocity is a key parameter for assessing the effectiveness of MICP in enhancing the stiffness of sand. However, one limitation of this study was the lack of a bender element transducer or resonant column test, which made it difficult to directly measure the shear wave velocity of the treated soil block. Another limitation is that the treated soil block height was only 12 cm, and the shear wave velocity obtained from the acceleration time histories yielded incorrect results. Therefore, we treated the soil in a Direct Simple Shear (DSS) mold. Following the treatment, the shear wave velocity and peak friction angle were measured. Then, the same treatment procedure was applied to a MICP-treated soil block, as shown in Figure 2a. After treatment, a direct shear test was performed with the same vertical stress to determine the peak friction angle. The friction angle obtained from the direct shear test for the MICP-treated block was compared with the friction angle measured using the DSS method, with the variation between the two methods being less than 1 degree. This finding indicates that the shear wave velocity measured via the DSS method was 250 m/s, which closely corresponds to that of the MICP-treated block.

(a)

(b)

Figure 2. (a) MICP treatment block, (b) Dismantle mold and treated soil

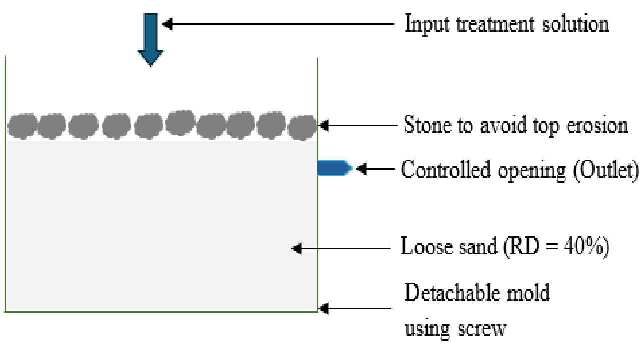

Figure 3: Schematic diagram of the injection procedure into the block

`

Figure 4. The placement of the MICP block into the model ground

In the previous discussion, the thicknesses of various soil layers were detailed as follows: the crust measured 12 cm, the liquefiable layer 26 cm, and the dense layer 20 cm. The groundwater level (GWL) was positioned 12 cm below the surface, which corresponds to the top of the liquefiable layer, as illustrated in Figure 1. Additionally, the treated soil block had a thickness of 12 cm. To incorporate the treated soil into the model ground, the thickness of the dense layer was reduced by 8 cm, while the crust layer was correspondingly increased by 8 cm, with the thickness of the liquefiable layer remaining unchanged. Upon completion of the model ground's preparation, the GWL was again located 12 cm from the surface, maintaining the same configuration. The transfer of the treated soil block was particularly challenging due to its brittle nature. To address this issue, the inner mold was removed after sample preparation, as illustrated in Figure 2b. The treated sample was then supported from the top on all sides, with the bottom of the holder left open, and carefully placed at the center of the model ground, as depicted in Figure 4. Additionally, the overall configuration of the model ground, including the MICP-treated soil, is illustrated in Figure 1. These figures provide a comprehensive visual representation of the treated and untreated sections of the model ground, highlighting the spatial arrangement and the modifications made for the inclusion of the treated soil block.

RESULTS AND DISCUSSIONS

Although the target acceleration and frequency were 0.53g and 6.68 Hz, respectively as given in Table 1, the achieved peak acceleration and frequency of the input motion during the shake table tests were 0.28g and 2.73 Hz. We conducted several shake table tests using a PGA of 0.28g with varying durations. A PGA of 0.28g with a shaking duration of 13 seconds can adequately represent the generation and dissipation of excess PWP, while shorter durations were insufficient to trigger liquefaction effects. Therefore, a shaking duration of 13 seconds was selected, consisting of a 6-second cyclic ramp-up phase followed by 7 seconds of uniform amplitude motion. To ensure the comprehensive capture of data, each test was recorded for a total duration of 30 seconds, allowing for the monitoring of acceleration, PWP generation and dissipation, and foundation settlement over time. The results obtained from the 1g shake table tests are analyzed in terms of the time histories of excess PWP ratio, and foundation settlements. These parameters provide key insights into the dynamic response of the model ground under simulated seismic conditions, offering a detailed understanding of how treated and untreated soil blocks behave during and after the shaking event.

Excess PWP time histories

Figure 5 presents the time histories of excess PWP beneath the foundation, specifically within the middle of the liquefiable layer (25cm below the surface), both with and without the application of mitigation measures. The locations of the PWP sensors are detailed in Figure 1. To quantify the liquefaction effects, the excess PWP ratio (R_u) was calculated. This ratio represents the proportion of excess PWP generated in a soil mass relative to the initial effective vertical stress. For calculating the initial effective vertical stress, the weight of the soil above the PWP sensor, the weight of the treated block, and the weight of the foundation and structure were all considered.

Figures 5a and 5b display the excess PWP ratio time histories for the foundation (F) and free field (FF), respectively. In Figure 5a, the excess PWP was generated uniformly and took a longer time to dissipate, indicating a slower recovery of soil strength in Test 1 (No Mitigation). The excess PWP ratio reached 1, signifying liquefaction and subsequent collapse of the structure during shaking. Conversely, in the MICP-treated soil block, the excess PWP ratio was less than 1, indicating that the liquefiable soil beneath the foundation did not liquefy during shaking. The dissipation of excess PWP occurred much faster—almost 50% quicker than in Test 1, as indicated by the double-headed arrow. This accelerated dissipation facilitated a quicker recovery of the soil's shear strength.

In Figure 5b, the excess PWP ratio time histories in the free field conditions for both tests were similar. However, a notable difference was observed during the dissipation stage, where the excess PWP ratio was higher in Test 2 than in Test 1. This can be attributed to the MICP treatment, which significantly reduced the permeability of the treated soil. During shaking, the lower permeability restricted the movement of water. Over time, the trapped water dissipated into the surrounding untreated areas, where the permeability was higher, allowing for a gradual release and redistribution of the water.

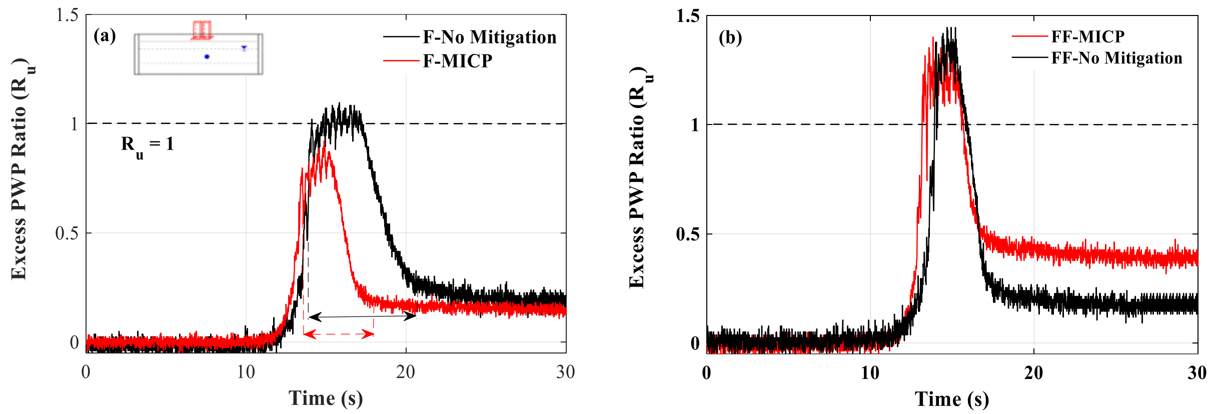

Figure 5. Excess PWP ratio time histories with and without mitigation measures (a) beneath the foundation (b) free field in the mid-liquefiable layer

Acceleration time histories

Figure 6 illustrates the acceleration time histories corresponding to various locations, including the input motion, soil layers at different depths beneath the foundation, the foundation itself, and the structure. The positioning of the accelerometers is depicted in Figure 1. The recorded accelerations at the base (input motion) and in the middle of the dense layer were nearly identical, indicating consistent transmission of seismic waves through these layers. However, within the middle of the liquefiable layer, acceleration was deamplified as it propagated upward through the soil column, reducing the motion by a factor of 0.82 due to partial liquefaction. Upon reaching the structure, the acceleration was amplified by a factor of 1.5. This amplification can be explained by the foundation positioned on top of the MICP-treated block which served as a base slab isolator. This isolator evenly distributed the building's load across the soil and enhanced stability while providing support by resisting compressive forces. As a result, liquefaction did not occur in the model and the entire system behaved elastically. The faster propagation of seismic waves through the MICP-treated soil compared to untreated soil resulted in amplified surface acceleration.

Foundation settlement time histories

Two LVDTs were mounted on the flat surface of the structure, as shown in Figure 1a, to measure its vertical displacement. The LVDT had a maximum range of 9 cm. During the shaking in Test 1 (no mitigation), the LVDT recorded a maximum of 9 cm, while the final settlement measured 11.40 cm after shaking. Based on the recorded settlement time histories from the LVDT and the final settlement, we interpolated the missing data in the foundation settlement time histories. This illustrates one of the limitations of the LVDT used in this study. Therefore, we have plotted the highest foundation settlement time history for Test 1 in Figure 7a. For Test 2 (MICP treated), the foundation settled vertically, resulting in similar foundation settlement time histories recorded in both LVDTs, as shown in Figure 7a. Based on these foundation settlement-time histories in Figure 7a, the maximum foundation settlement was determined. This maximum foundation settlement is then plotted against the mitigation measure in Figure 7b.

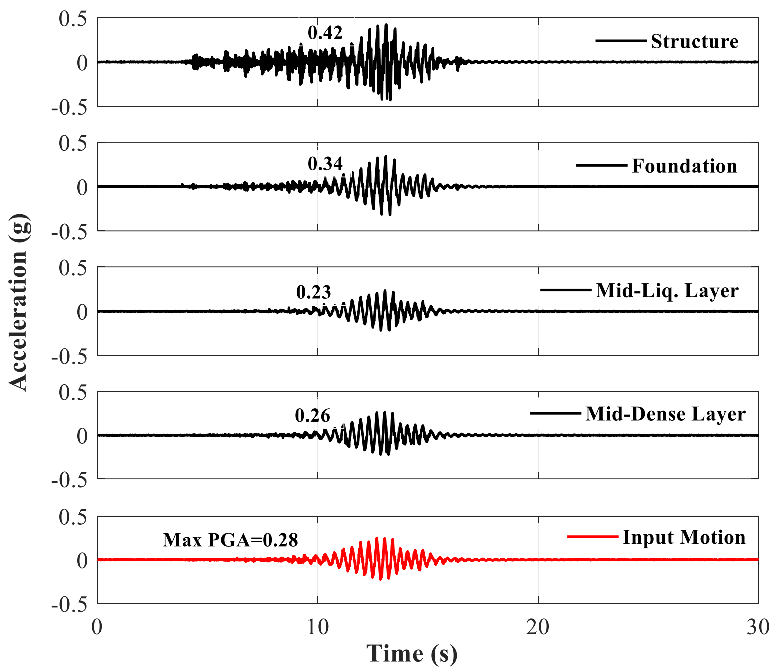

Figure 6. Acceleration-time stories at the different soil layers for MICP treated soil

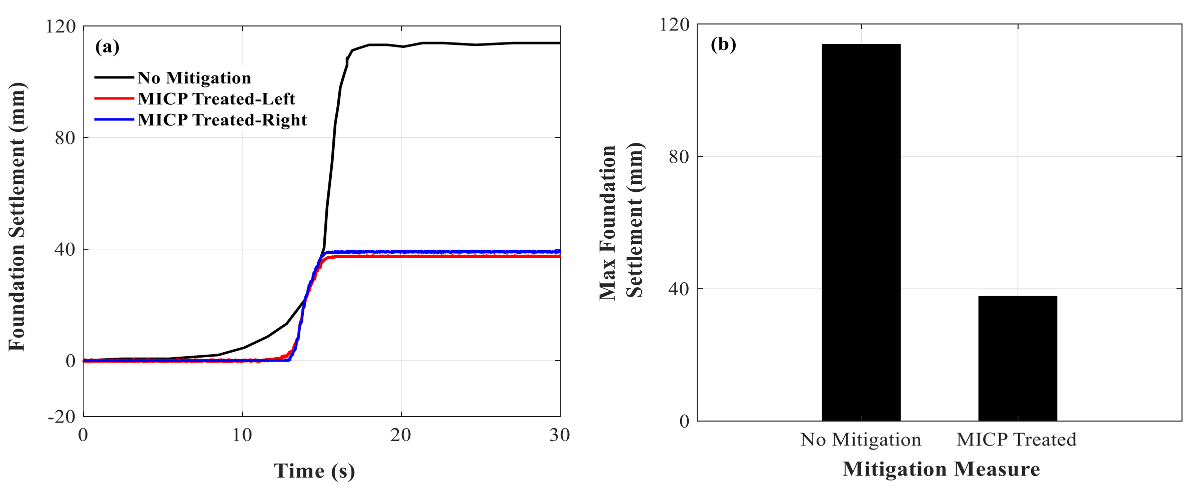

Figure 7. (a) Foundation settlement-time stories (b) The variation of maximum foundation settlement with and without mitigation measure

In calculating the maximum foundation settlement, the total settlement was considered, defined as the cumulative foundation settlement that occurs both during and after the seismic shaking event. This comprehensive approach provides a clear assessment of the overall impact of seismic activity on foundation stability. Notably, in Figure 7b, the application of MICP reduced foundation settlement by 64%. This significant reduction can be attributed to the treated soil block beneath the foundation, which acted as a base slab isolator. The treated soil block deformed under seismic pressure, absorbing much of the earthquake's energy and mitigating the swaying and shaking of the structure, thereby reducing the overall impact of seismic forces on the foundation.

Figure 8 visually illustrates the liquefaction-induced foundation settlement observed during the tests. The configuration of the model ground is shown in Figure 8a. To assess differential settlement, measurements were taken at the four corners of the foundation both before and after the seismic shaking. The longitudinal directional tilting was calculated by dividing the differential settlement by the length of the foundation, while the transverse directional tilting was calculated by dividing the differential settlement by the foundation's width.

(a) Before Shaking

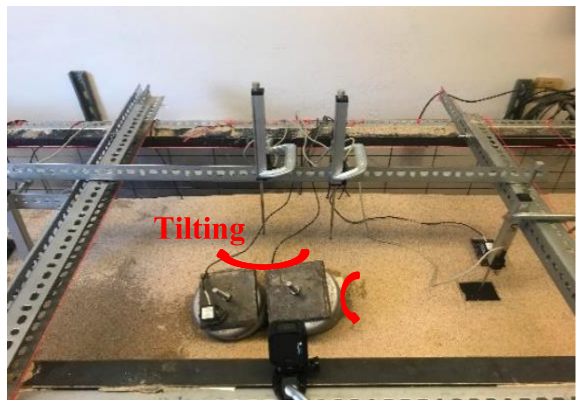

(b) No mitigation

(c) MICP Treated Soil

Figure 8. Observed foundation settlement and tilting after shaking

In Figure 8b, it is evident that the transverse directional tilting was greater than the longitudinal directional tilting. The difference occurred because shaking in the longitudinal direction caused tension in the soil at the foundation corners, leading to greater settlement in the transverse direction. After the application of MICP treatment, the foundation exhibited elastic behavior and settled primarily in a vertical direction. As a result, the transverse directional tilting was eliminated by 96%, and the longitudinal directional tilting was also reduced by 95%. This outcome demonstrates the effectiveness of MICP in mitigating differential settlement and reducing foundation tilting under seismic loading.

The difference between previous centrifuge tests and our study is the design of the MICP-treated block. While San Pablo (2024) and Ham et al. (2024) employed discrete blocks measuring 10 cm × 10 cm × 15 cm, covering 37% of the liquefiable soil depth, our study used a 26 cm × 12 cm × 12 cm block designed to cover the "B" distance beneath the foundation. Ham et al. (2024) positioned the structure above the aforementioned MICP-treated block, achieving a 54% reduction in structural settlement. Despite variations in PGA, shaking duration, and soil properties, both studies highlight the effectiveness of MICP in reducing liquefaction-induced foundation settlements.

CONCLUSION

Two 1g shake table experiments were conducted to investigate the effectiveness of MICP in mitigating liquefaction-induced foundation settlement. The model ground was subjected to the same input motion in both tests. Based on the experimental results, the following conclusions were drawn:

- The application of MICP-treated soil block in the ground model reduced the duration of excess PWP generation and dissipation by 50%.
- The acceleration was amplified by a factor of 1.5 from the input motion to the structure.
- The incorporation of the MICP-treated soil block altered the ground model's geometry, resulting in a 64% reduction in foundation settlement and a 95% reduction in foundation tilting.

This investigation focused on the use of a single treated soil block as the primary mitigation measure. In future research, varying the size of the treated soil block will be considered to deepen the understanding of its effectiveness in mitigating liquefaction-induced effects in liquefiable soils.

ACKNOWLEDGMENTS

This work was supported by funding through the GAANN Fellowship which stands for Graduate Assistance in Areas of National Need, which is a program sponsored by the U.S. Department of Education. I would like to express my gratitude to Dr. Jason T. DeJong for his valuable guidance on the MICP test procedure.

REFERENCES

Alam, M. K., Zogh, P., Yazdi, M., and Motamed, R., (2023). “Effect of shaking duration on foundation settlement in liquefiable soils: 1-g shake table tests.” *In Geo-Congress* 2023, pp. 89-98.

Alam, M. K., and Motamed, R., (2024). “Experimental evaluation of optimizing sheet pile installation depth and distance to mitigate liquefaction-induced foundation settlements.” *DFI Journal-The Journal of the Deep Foundation Institute*, Vol 18, Issue 1, 1-15.

Das, B. M., and Sivakugan, N., (2018). *Principles of foundation engineering*. Cengage learning, Inc. 200 Pier 4 Blvd, Ste 400, Boston, MA 02210, US.

Darby, K. M., Hernandez, G. L., DeJong, J. T., Boulanger, R. W., Gomez, M. G., and Wilson, D.

W., (2019). "Centrifuge model testing of liquefaction mitigation via Microbially Induced Calcite Precipitation." *Journal of Geotechnical and Geoenvironmental Engineering*, 145 (10), 04019084.

Ecemis, N., Karaman, M., Valizadeh, H., Dönmez, C., and Dalgıç, K. D. (2023). "Soil liquefaction and effects on structures; case study in Adıyaman-Gölbaşı after the 06 Feb 2023 earthquakes in Türkiye." *7th International Conference on Earthquake Engineering and Seismology,* 6-10 November 2023 in Antalya, Türkiye, pp 1-12.

Ham, S. M., San Pablo, A. C., Caisapanta, J. L., and DeJong, J., (2024). "Centrifuge modeling of soil-structure interaction with MICP improved soil." In *Geo-Congress 2024*, pp. 87-95.

Iai, S., (1989). "Similitude for shaking table tests on the soil-structure fluid model in 1g gravitational field." *Journal of Soils and Foundations,* Vol. 29, No. 1: 105-118.

Ishihara, K., Araki, K., and Kamata, T. (2014). "Liquefaction 1 in Tokyo Bay and Kanto regions in the 2011 Great East Japan Earthquake." *Earthquake Geotechnical Engineering Design*, *Springer*, 93-140.

Montoya, B. M., Dejong, J. T., and Boulanger, R.W. (2013). "Dynamic response of liquefiable sand improved by microbial-induced calcite precipitation." *Geotechnique*, 63 (4), 302–312.

Naeimi, M., and Haddad, A., (2018). "Investigation on the environmental impact of soil improvement techniques: comparison of cement grouting and biocement." *In Proceedings of GeoShanghai 2018 International Conference: Geoenvironment and Geohazard. GSIC May 27 – 30, 2018.* Springer, Singapore, page 483-490.

Orang, M. J., Motamed, R., Prabhakaran, A., and Elgamal, A., (2021). "Large-scale shake table tests on a shallow foundation in liquefiable soils." *Journal of Geotechnical and Geoenvironmental Engineering*, 147(1), 04020152.

San Pablo, A. C., DeJong, J. T., and Carey, T. J. (2024). "Influence of biocementation treatment extent on dynamic system performance: A centrifuge liquefaction study." *Soil Dynamics and Earthquake Engineering*, *183*, 108792.

Toth, J., and Motamed, R., (2017). "Parametric study on liquefaction-induced building settlements using 1-g shake table experiments." *The 3rd International Conference on Performance Based Design in Earthquake Geotechnical Engineering, Vancouver, CA, July* 16-19 2017, Paper no. 149.

Zamani, A., Xiao, P., Baumer, T., Carey, T. J., Sawyer, B., DeJong, J. T., and Boulanger, R. W. (2021). "Mitigation of liquefaction triggering and foundation settlement by MICP treatment." *Journal of Geotechnical and Geoenvironmental Engineering*, 147(10), 0402-1099.